

Analysing the Isotopic Composition of Atmospheric CO₂ in Urban Areas

Rafat Ahmed
Supervisor: Dr Heather D. Graven

02/10/2020

A thesis submitted in fulfilment of the requirements for the degree of MSc Physics and the
Diploma of Imperial College London

Declaration of Work

As a predominantly computational project, much of my work and analysis was completed via Python. All figures, unless explicitly referenced in the figure caption, have been produced from the data collected by Imperial College London, by myself using Python 3.8. Any and all mathematical derivations and formulas have been taken from past literature and referenced accordingly. I have written this report myself and maintained good academic conduct to the best of my ability and cited any work that is not my own.

Contents

Acknowledgments	4
Abstract.....	5
1. Introduction.....	6
1.1 Project Background and Aims	6
1.2 Carbon Dioxide Emissions in London	7
1.3 Isotopic Source Signatures of CO ₂	8
2. Data Analysis of Atmospheric CO₂	9
2.1 CO ₂ Data from the Huxley Building.....	9
2.2 Keeling Plot Analysis.....	10
2.3 Data Processing	12
3. Results	14
3.1 Findings from the Keeling Plot Analysis	14
3.2 Time-Series Analysis of Source Signatures	17
3.3 Analysis of the Lockdown Period	20
3.4 Wind Data Analysis	22
Conclusion	25
Outlook.....	26
References.....	27

Acknowledgments

This project was completed under the supervision of Heather Graven. I wish to thank Heather for providing me with the opportunity to work on the project and investing time into frequent meetings throughout the summer to address any queries, clarifying issues and just generally ensuring the project ran as smoothly as possible amongst the midst of a global pandemic. I would also like to extend my gratitude to Giulia Zazzeri and Eric Schoenrock for their committed advice and for taking time out of their busy schedules to assist with issues in my work. Overall, I enjoyed the challenges and experience of this project and developed life-long skills along the way. It has been one of the main highlights of my master's degree and I thank Heather, Eric and Giulia for making it such a beneficial experience.

Abstract

Afternoon Carbon dioxide data collected between 2018-2020 from the South Kensington campus of Imperial College London was analysed to understand the variations observed in the isotopic source signatures of CO₂ in London and the processes contributing to them. Results from the Keeling plot analysis method deployed to calculate isotopic source signatures, showed that the most dominating source of anthropogenic CO₂ in London was from a mixture of sources as a result of natural gas combustion, with the average isotopic signature corresponding roughly to $36.8 \pm 0.5\%$. Analysis of the data using 1-day, 3-day and 7-day afternoon time windows were carried out and the results revealed that a clear seasonal variation was observed in the source signatures over time. Time series analysis of the isotopic signatures generally showed agreement with other studies conducted in urban regions, with greater variability of $\delta^{13}\text{CO}_2$ in the summer than the winter. Winter periods exhibited phases of heavier signatures with an average value of $-37.6 \pm 0.4\%$ relative to summer periods with average values found to be $-34.4 \pm 0.6\%$. From the analysis of the calculated isotopic source signatures, it was found that the most influencing factors behind these differences were due to the cyclical nature of temporal variability throughout the seasons and the resulting influence from biospheric emissions and the combustion of fossil fuels for domestic heating. In an attempt to better understand this variation, wind direction data was analysed, and the findings suggested that overall, natural gas combustion signatures appear to be originating almost evenly between eastern and western regions.

1. Introduction

1.1 Project Background and Aims

Carbon dioxide accounts for the largest proportion of anthropogenic greenhouse gases in the atmosphere, with urban regions contributing more than 70% of global CO₂ emissions resulting from fossil fuel combustion alone [1]. Urban areas such as cities and towns worldwide, are found to be net sources of CO₂ despite accounting for only 0.4-0.9% of land surfaces [15]. Aside from water vapour, CO₂ is the most significant greenhouse gas that has been driving climate change over the past decades. Studies into atmospheric CO₂ have aided researchers in understanding the balance between emissions arising from human activities and that which is taken up by Earth's reservoirs. Understanding this balance in CO₂ concentration allows researchers to constrain the sources and sinks of CO₂ that are known to exist.

The main goals of this project were to identify the most dominating sources of CO₂ found from the measurements and quantifying the relative contributions of major anthropogenic and biospheric sources to the local atmosphere, by combining the concentration and stable isotope measurements to trace CO₂ pollution events back to a source. As well as this, the project also aimed to establish the potential causes behind the variations found in the isotopic source signatures over time. To achieve this, the project focused on analysing the afternoon data between 12pm and 5pm.

Several research projects exist that have utilised Keeling plot analysis to understand the isotopic signature variations of atmospheric CO₂ in urban areas and quantify the most influential sources of CO₂. One such study was carried out in Florence, Italy, where carbon isotopic ratios were used to infer sources and sinks of CO₂ by analysing the diurnal variations of greenhouse gases. The results presented by Venturi et al in Florence found that petrol combustion was the most influential source of CO₂ that was causing the city of Florence to act as a net source of CO₂ [5]. A similar study carried out in 10 separate sites across Paris using the isotope tracing technique to sample atmosphere CO₂, also found that the combustion of petrol from road traffic was the predominant source of CO₂ measured from a few meters above ground level [21]. This was also the case for the results in Florence, where the majority of CO₂ pollution sources were related to vehicle traffic and domestic heating. Another study conducted in Kraków, Poland found a definitive seasonal pattern of $\delta^{13}\text{C}_{\text{CO}_2}$ with more stable but heavier source signatures during the winter relative to the varied lighter signatures found during the summer and spring [20]. Their research appeared to show the dominance of biospheric emissions during the summer, whilst during the winter anthropogenic source of CO₂ were more prominent. Many of these studies however, differed in the mass-balance models used to distinguish between the emissions from anthropogenic and biogenic source of CO₂, which each bring with it their own set of uncertainties and differences. Kraków et al utilised a three-component mixing model, whilst the measurements found from Widory et al in Paris were based on a binary mixing model. In this project, a two-component mixing model was used, where the two components were the background CO₂ emissions and the second component being the CO₂ emissions from the sources directly. It is important to note that in these studies, atmospheric CO₂ data was analysed over shorter time periods extending over a few weeks and months. On the other hand, this project examined the variations of the isotopic source signatures in atmospheric CO₂ samples during the afternoon, from data over a period of 2 and a half years between 2018 and 2020.

This report begins first by introducing the methods of analysis used throughout the project in section 2. Details about the measurement procedures and purposes are briefly explained in

section 2.1, with section 2.2 and 2.3 detailing much of the early data analysis work that was involved in constructing Keeling plots to obtain source signatures of pollution events. Section 3 provides an overview of the key results found from the analysis performed, where section 3.1 summarises some of the findings from the generated Keeling plots over the different time windows. Section 3.2 presents the variation of the isotopic source signatures over the whole period of 2018 – 2020. Section 3.3 analyses the effects of the nationwide lockdown implemented during the spring of 2020 to better understand the trend in the source signatures and interpret how human behaviour could possibly be impacting the seasonal cycles. Section 3.4 briefly discusses the results obtained from analysing the recorded wind direction data and the effects wind conditions have on the distribution of observed sources signatures.

1.2 Carbon Dioxide Emissions in London

Many campaigns and initiatives for the continuous measurements of atmospheric CO₂ have been recorded, namely by the National Oceanic Atmospheric Administration (NOAA) in the US since 1958, yet not many of these records address the emissions generated by urban regions specifically. Since late 2017, the Space & Atmospheric research group have been collating data on carbon dioxide and methane concentrations via a weather station located on the Huxley building, 2.6 miles from central London. The UK as a whole emitted 451 million tonnes of greenhouse gases in 2018, of which 366 million tonnes was due to CO₂ emissions, representing a 43% and 39% decrease from 1990 levels respectively [3]. The main driver behind these immense changes has been the gradual shift away from the use of coal as a primary source of energy across the globe, driven by national and international climate agreements. Policies implemented by the UK government including the introduction of low-emission zones around London and the Climate Change Act of 2008 have further contributed to the reduction of coal combustion for energy.

Measurement campaigns in London aimed at assessing isotopic source signatures of CO₂ have taken place at Royal Holloway University, located 23 miles from central London and at King's College London. The longest in-situ measurements of atmospheric CO₂ in London were conducted at Royal Holloway University lasting 13 years, from 2000 to 2012. Analysis of this data were able to show daily and 30-minute seasonal cycles of carbon dioxide mole fractions, which exhibited maximum concentrations during the winter and the lowest concentrations during the summer, instigated by temperature, vegetation, combustion emissions and meteorology [23]. The monthly averages of the results calculated by the researches indicated that total CO₂ concentrations observed at their measuring site in Egham increased incrementally by 28ppm on average, significantly higher than that calculated for the background concentration measured at Mace Head at 22ppm – confirming the results seen from other sites worldwide of increasing CO₂ concentrations.

1.3 Isotopic Source Signatures of CO₂

The three naturally occurring isotopes of carbon are ¹²C, ¹³C and the unstable isotope ¹⁴C, which is used for radiocarbon dating for fossils. The carbon present in atmospheric CO₂ therefore contains traces of these carbon isotopes at different proportions varying by region. Due to each carbon isotope containing its own unique identification, a method of isotope tracing can be utilised to distinguish between the exact constituents of CO₂ present in a given sample of air [4]. In this instance, the use of ¹³C isotopes to identify local sources of CO₂ was implemented by looking at the proportion of ¹³C relative to ¹²C in the ambient air arriving at the sensor. The ratio, $\delta^{13}C$ represents the isotopic source signature and is given by:

$$\delta^{13}C = \left(\frac{R_{sample}}{R_{standard}} - 1 \right) \times 1000\text{‰} \quad (1)$$

Where the standard molar fractions of an air sample, $R_{sample} = (^{13}C/^{12}C)_{sample}$ and $R_{standard} = (^{13}C/^{12}C)_{standard}$ with the standard ratio referring to an established reference for the ratio of ¹³C to ¹²C – this is the Vienna Pee Dee Belemnite (VPDB) scale for the data. As established by the International Atomic Energy Agency, the VPDB value of 0.0111802 ± 0.000016 [27] for was used throughout the calculations for the source signatures throughout this project.

Table 1 shows the major sources of atmospheric CO₂ contributing to measurements and the corresponding approximate signature. This was drawn up from the values stated across a combination of papers studying $\delta^{13}C$ measurements across different urban locations. As would be expected, the values of these isotopic signatures are subject to variability and are quoted as such in their respective papers. There is a degree of discrepancy found in the literature between isotopic signatures of different sources due to the lack of precisely constrained values of contributions from different sectors, which are mostly affected by location and weather condition factors. The construction of table 1 above reflects this by quoting the different sources by a range.

The different sources of CO₂ lead to different $\delta^{13}C$ values due to the differing amounts of carbon-13 content in the sources. This is due to the degree of fractionation of carbon isotopes within different carbon reservoirs during combustion and chemical processes, where a carbon-isotope fractionation reaction will favour either of the stable carbon-13 or carbon-12 isotopes as the end product [18]. The variations in these reactions tend to leave different sources with a different fractionation factor and different proportions of end products, which leads to distinct isotopic source signatures being found for specific combustion processes. For example, it was shown in the carbon isotope studies in Paris [21] that signatures from diesel vehicles and those that used leaded fuel varied due to different CO₂ content and the different combustion processes involved depending on the vehicle type.

Source	Isotopic Signature (‰)
Natural Gas Combustion	-45 – -33
Petrol Combustion	-32 – -31
Plant Respiration	-30 – -26

Table 1: Approximate range of values for $\delta^{13}CO_2$ drawn from different sources of atmospheric CO₂ collated from various literature [16][17][20][21].

Carbon dioxide sources are essentially characterised based on specific $\delta^{13}\text{CO}_2$ signatures, so by analysing stable isotope ratios of atmospheric CO_2 samples the contributions from different urban sources can be distinguished – implementing an isotope tracing technique in this way also allows for the urban processes observed to be partitioned into their distinct components.

CO_2 emissions from urban regions are typically measured through the use of a bottom-up approach, which is based on calculating the emissions found from individual sectors within a defined area and summing up the individual contributions to obtain the total emissions for the whole region; essentially calculating the emissions in a source-by-source basis to obtain the aggregate emissions [19]. Use of bottom-up inventories are found to be time consuming and requires a vast amount of data to estimate emissions independently. Top-down inventories on the other hand, utilise inverse modelling of CO_2 mixing ratios to determine CO_2 sources, which often requires measurements to be taken at high spatial resolution typically by aircrafts and then distributed over the modelling domain. For urban measurements, emission inventories are found to rely more upon bottom-up methodologies however, both techniques produce divergence in the emission estimates they produce and instead a more common approach is to combine top-down and bottom-up inventories into a single inventory [24].

2. Data Analysis of Atmospheric CO_2

2.1 CO_2 Data from the Huxley Building

The measurement site located 24m above ground level, at Imperial College London was used to collect carbon dioxide fluxes from different sources. The main goal of this was to develop and compare atmospheric CO_2 models against the observed measurements to identify the dominant sources that are contributing to CO_2 emissions around London. From this, estimates of CO_2 fluxes can be better predicted and atmospheric transport models of CO_2 better developed by using data from observations as a constraint for the models [13].

The sensor utilises an isotope ratio mass spectrometer which samples air arriving at the sensor location at 1-minute intervals, with the mass of the constituents present in the air from which the isotopic source signature can be inferred from. The weather station includes an air inlet that is connected to instrumentation in the laboratory that allows the ambient air to be measured from which the atmospheric models are able to be constructed. Alternative methods of identifying sources of CO_2 involve using specific tracers such as carbon monoxide [14], which is a by-product of different combustion processes, but issues have been raised around the inaccuracy with which tracing techniques such as these bring when constraining CO_2 sources and sinks.

The atmospheric models developed work by tracing the journey of air samples arriving at the weather station, which can then be run by emitting particles from the sensor location and tracking their route back to the origin of the emitting region. This process of combining CO_2 observations along with atmospheric transport models allows researchers to verify other bottom-up inventories, such as NAEI and EDGAR which ultimately assists governments monitor greenhouse gas emissions more effectively to measure how well regulations and agreements are being implemented as well as allowing for government policies to be independently tested. Throughout this project, the isotope measurements and concentration measurements were coupled together in trying to determine the relative contributions of different CO_2 sources in London.

2.2 Keeling Plot Analysis

Through the construction of Keeling plots, the isotopic source signatures of observed CO₂ pollution events were identified. Keeling plot analysis is a method of interpolation, allowing for the mean isotopic source signature of a signal that is mixed into a background reservoir to be determined from the observed isotopic composition and mole fraction [2]. A similar approach taken by Thomas Röckmann et al in defining distinct time windows was adopted in generating estimates for source signatures from Keeling plots **[Error! Reference source not found.]**. Data within time windows of 1-day, 3-day and 7-day lengths, between 12pm and 5pm were analysed. This was chosen to understand how the build of afternoon CO₂ varied across longer time frames and to try and distinguish the anthropogenic sources of CO₂ from biogenic sources. During the afternoon, it is expected that the active anthropogenic CO₂ sources are likely to contribute more significantly to total emissions and it is this accumulation that was of interest to identify the major sources of human-induced CO₂ detected by the sensor.

Due to the stability of wind conditions during the night and generally stronger winds over diurnal periods, the planetary boundary layer tends to be at its peak height during the daytime and at its lowest position overnight[11], which leads to the entrapment of CO₂ emissions from more local sources at night time. This has the effect of pronouncing these local signals over more regional sources when looking at the data over short periods less than 24 hours. Over diurnal periods, varied winds at higher speeds cause the accumulated CO₂ from the boundary layer overnight to disperse. So, by looking at the afternoon data only, we are able to understand the effects of atmospheric transport on the dispersion of wider CO₂ sources being detected. In addition to the 1-day afternoon window, 3-day and 7-day windows were also used. The reason for this was that studying afternoon data over a larger range allowed a greater build-up of CO₂ to be observed, which may not have been as apparent in the 1-day window alone.

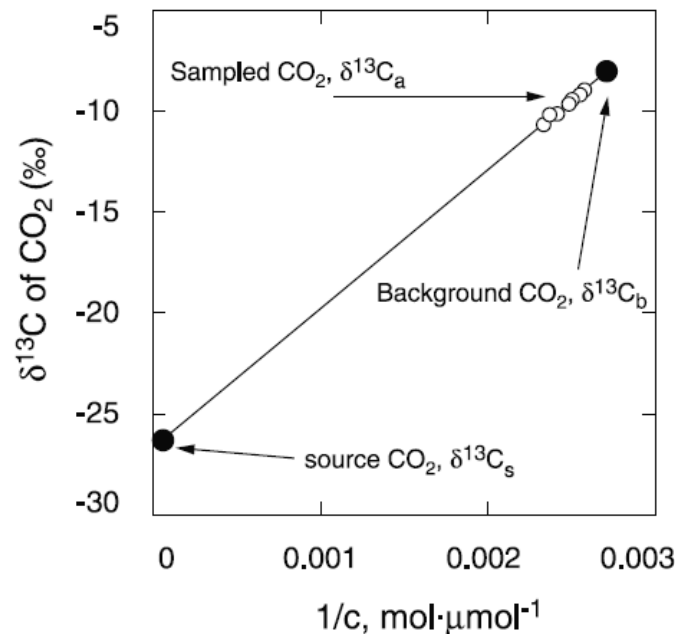


Figure 1 [6]: The Keeling plot technique involves interpolating between two carbon isotopic composition points, with the first representing the CO₂ source – $\delta^{13}\text{C}_s$ and the last point representing the background CO₂ – $\delta^{13}\text{C}_b$. In this example, the measurements of the sampled air are denoted by the white circles. This describes how the isotopic signature of the source in equation (3) is then obtained from the intercept of the linear regression line.

The use of longer time windows over several days also allowed a greater area of influence to be studied, meaning that the influence from sources on a larger scale could be seen and the variations of signals from regional influences could be understood. Longer time windows essentially represent an extended travel log of ambient air arriving at the weather station, enabling the data to be tracked back further and possibly closer to the source.

There are inherent assumptions that accompany the Keeling plot analysis method, which include a constant background concentration of CO₂ and a build-up of CO₂ emissions directly from sources over a specified observation period – looking at afternoon periods ensured that this was satisfied as best as possible, but not perfectly. Since the concentration from a sample of gas of atmospheric CO₂ contains a combination of background concentration and additional concentration from different sources within the atmosphere, the Keeling plots were constructed on the basis of a two-component mixing model, as expressed through the mass balance equations. Adopting the same approach as Venturi et al (first devised by Charles D. Keeling [7]) in their study of the seasonal variation of greenhouse gases in Florence, the isotopic signature can be derived from the concentration and isotopic composition mass balance equations of the background and sources [5]:

$$C_m = C_b + C_s \quad (2)$$

$$\delta^{13}C_m \cdot C_m = \delta^{13}C_b \cdot C_b + \delta^{13}C_s \cdot C_s \quad (3)$$

and expressed via the following expression:

$$\delta^{13}C_m = \frac{(\delta^{13}C_b - \delta^{13}C_s) \cdot C_b}{C_m} + \delta^{13}C_s \quad (4)$$

Where the values for the measured, background and sources are represented by the subscripts m , b and s . Equation (4) describes a straight line on a plot of $\delta^{13}C$ against the inverse of the total measured CO₂ concentration in the form $y = m/x + c$, with the intercept of this line corresponding to the source signature, $\delta^{13}C_s$ as detailed in figure 1. The limit in which the $\delta^{13}C$ is zero, the total CO₂ would be infinite – this point therefore represents the isotopic signature of the source, as if the total CO₂ concentration in the sample originated from the source. It was not necessary to explicitly calculate the delta value of the background since this is assumed to be constant, which ultimately simplifies the problem. This is not always the case however, as it is expected for the isotopic signatures of each single CO₂ source to vary overtime. Classifications of the calculated source signature values obtained were based off the values provided in table 1.

2.3 Data Processing

This section covers the processes involved in setting up the initial calculations performed on the CO₂ measurements and how they were carried out.

As outlined in [6], there are significant differences between a Model I and Model II linear regression method. Model II regression procedures account for uncertainties in both the dependent and independent variables, whilst a Model I fit assumes that only errors on the dependent variable are significant – resulting in a systemic bias in the estimates of the slope and intercept. An Ordinary Least Squares Model I fit for example, brings with it some issues when implementing it on our dataset. OLS fitting treats variables as though they are not subject to any kinds of errors and requires the dependent variable to be an explicit function of the independent variable, which was not quite possible given the nature of the data being studied. Generally, Model I regression is found to underestimate the value of the slope for a linear relationship between two variables [28] and since both the CO₂ concentration and $\delta^{13}\text{C}$ variables were not controlled, a Model II orthogonal distance regression fit was used to construct Keeling plots for this project. To achieve this, the odr function from the scipy package in Python was utilised, which is based on the Levenberg-Marquardt algorithm to minimise the perpendicular distance between the fit and datapoints [12].

To make this procedure more computationally efficient, initial fit parameters for the slope and intercept were provided from calculated values using an OLS fit, which were estimated via the scipy.polyfit function. This was to ensure the convergence of the regression line produced by scipy.odr and that the function did not overshoot and take a long time to process the result. ODR fits also require initial estimates for the errors on the dependent and independent variables of the data, which was achieved by calculating the standard deviation for the $\delta^{13}\text{C}$ and the inverse total CO₂ concentration using the statistics.stdev function. This process of ODR fitting technique was applied to each time window used for the data, filtering out the relevant source signature value based on statistical constraints placed on the Keeling plots. These conditions were for the regression line to have a goodness of fit parameter, R^2 greater than or equal to 0.8. The goodness of fit represents the accuracy of which a specific model fits observed data and ranges between 0 and 1, with 1 representing perfect agreement between the model and the sampled data. The goodness of fit parameter was also generated via the scipy.odr function as the residual variance, from which the goodness of fit can be found by, $R^2 = 1 - RV$ where RV is the residual variance. A second statistical constraint placed on the results was for the p-value to be less than 0.01. The p-value parameter acts as an indicator as to how well the predicted model would hold against a larger sample of data and tests the null hypothesis of the model. Setting a p-value criterion of ≤ 0.01 implied that the fitted regression model is producing somewhat meaningful results.

Total CO₂ concentrations for the data were calculated simply from the sum of carbon-13 and carbon-12 of measured CO₂ from the dataset. Since measurements of ¹²CO₂ were already recorded only the ¹³CO₂ needed to be calculated, which was done by rearranging equation (1) for ¹³C and using the standard value of 0.0111802 and taking the sum of the corresponding ¹³CO₂ and ¹²CO₂ values to obtain the total CO₂ value. When generating the Keeling plots, baseline data retrieved from measurements recorded in Mace Head were used as the background CO₂ concentration. This was due to the prevailing wind direction in Britain originating from the west and the Atlantic Ocean and as such the measurements from Mace Head offer a good background concentration for the London measurements to be compared against. Another criterion imposed on the Keeling plots was for the measured CO₂ concentrations below the baseline concentration to be filtered out when constructing the Keeling plots, which was implemented to ensure that only CO₂ emission generated from regional and local sources were being used. The total CO₂ from the measurements were found

to vary from between 393ppm and 692ppm, whilst the baseline CO₂ measurements ranged between 346ppm and 418ppm. However, no upper bound constraint was applied on the measured CO₂ concentrations used in the construction of the Keeling plots. A total of 395 Keeling plots were generated from the whole set of measurements between 2018 and 2020, across all three of the time windows and all Keeling plots were used in the results presented in these results.

3. Results

The 1-minute resolution data used throughout this project spanned from January 2018 to June 2020 and this project involved a broad analysis of the measurements collected for which the results are presented in this section. Section 3.1 summarises the isotopic source signatures found from the use of Keeling plots over the different time windows. Section 3.2 investigates the cyclical nature of the observed signatures and the potential causes behind them. Section 3.3 analyses the lockdown period to highlight any key differences found in the observed trends from 2018 and 2019. Section 3.4 looks at a possible relationship between wind direction and measured source signatures, both locally and regionally. It should be noted that only half the measured CO₂ data was available for the year 2020 but clear patterns were identified, and all observations and conclusions were drawn with this in mind.

3.1 Findings from the Keeling Plot Analysis

The mechanisms behind the Keeling plot technique was introduced in section 2.2 and shown explicitly in figure 1. Using an ODR fitting procedure, Keeling plots were generated for 3 different time windows for afternoon periods (12pm – 5pm) and the results used to interpret the variations found in the isotopic signatures. Initially, afternoon data from just 1-day windows were analysed, however additional 3-day and 7-day windows were later implemented to understand the influence of atmospheric transport on the air samples and the variations observed in the build-up of CO₂ concentration beyond local emissions. Figure 2 shows an example of three separate Keeling plots representing a different detected pollution event for each of the three windows. This involved constructing Keeling plots from the data contained within each of these windows, such that a 3-day window for example, would include all the 1-minute resolution datapoints every three day periods from which the Keeling plots would be filtered out based on the statistical criteria mentioned in section 2.3. This process was repeated for all the time windows used, with a total of 210 Keeling plots generated from the 1-day time windows, 126 for the 3-day windows and 59 for the 7-day windows. The goodness of fit and the isotopic source signature, C are both stated on each Keeling plot, where the signature value is quoted with the associated uncertainty value. As was done in [14], the standard deviation in the isotopic source signatures from a given sample were used to represent the uncertainty on the calculated $\delta^{13}C$.

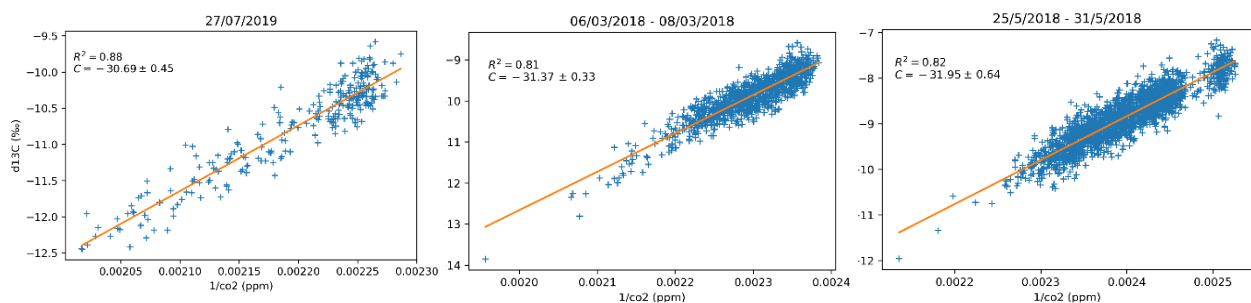


Figure 2: Representative Keeling plots of three different pollution signals. From left to right, the 1-day, 3-day and 7-day windows all show the calculated source signature of the corresponding event denoted by the intercept C , in units of per mil. The R^2 value quantifies the how accurately the regression line fits the observed data.

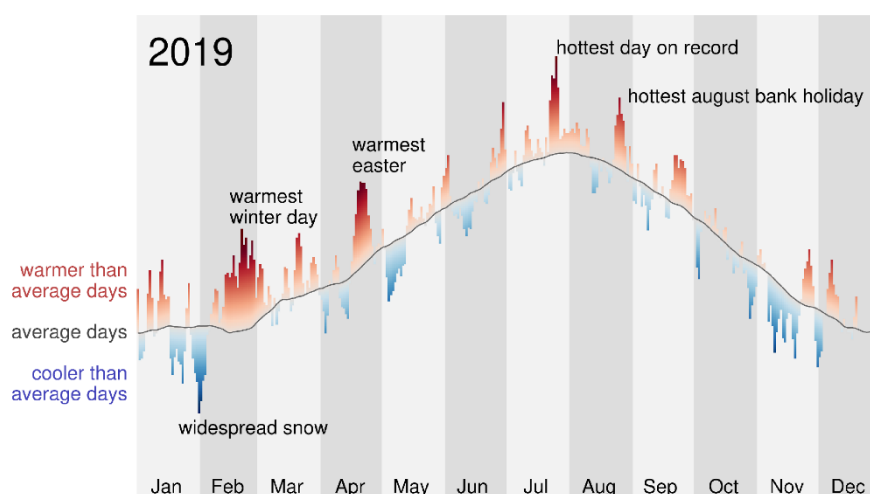


Figure 3 [10]: Time-series of average temperatures throughout 2019, which recorded several days with above average temperatures in the UK which was a potential cause of increased emissions due to biospheric influences

A summary of the isotopic source signatures identified in the 1-day and 7-day windows are shown in figure 4a and figure 4b. The distribution of the source signatures for each year show that the average value for the results between 2018 and 2020 appear centred around -38.7‰ for the 1-day window and 36.1‰ for the 7-day window – both of which correspond to sources originating from the combustion of natural gas. A notable feature of both plots in figure 4 is the slight shift of the 2019 peak source signature toward lighter signatures relative to 2018 and 2020. A possible cause for this could be attributed to the greater influence of plant respiration throughout 2019. The summer and spring periods of 2019 were found to have higher average temperatures across the UK, as illustrated in figure 3 by the Met Office review of 2019 [10]. Results from Frantz et al showed that for a 10°C increase in temperature, the corresponding rate of cellular respiration increased by 20% – 46% [8], which would likely have the effect of a greater contribution to the results found towards lighter signatures in 2019. This is more prevalent in the 1-day window of figure 4b. Longer time windows over a few days have a larger area of influence due to the observed variations associated with how air parcels travel over these longer periods before reaching the measurement site. As a result, the shorter windows of 1-day lengths are likely to be less impacted by the movement of air and so, results found in the 1-day window mostly represent signals from more local sources of CO_2 contributing to the emissions. For example, the proximity of local plant life around the campus and Hyde Park to the weather station would amplify these observations and would explain the shift towards lighter signatures observed in a 1-day window. This can be seen further in the first Keeling plot shown in figure 2, where the mean source signature during the warmest period of 2019 resulted in a $\delta^{13}\text{C}$ of 30.69‰ – significantly lighter than the average of 2019, $-38.4 \pm 0.9\text{‰}$. Lower signatures from the combustion of petrol from nearby busy highroads would also strongly influence the observed signals and it is likely that we are seeing a mixture of these sources contributing to local emissions. However, Keeling plots constructed for 1-day windows and shorter timeframes generally, are likely to be less precise as they tend to be more exposed to higher levels of scatter due to the varied wind conditions that accompany diurnal periods over a short timeframe. This appears to be contradicted by the results from figure 4b where over the longer 7-day window, the average signature value is lighter than that found over the 1-day window and a significant contribution from lighter signatures can still be observed, which

might suggest that the biosphere has a much larger overprint on the isotopic signatures during the afternoon than was initially thought.

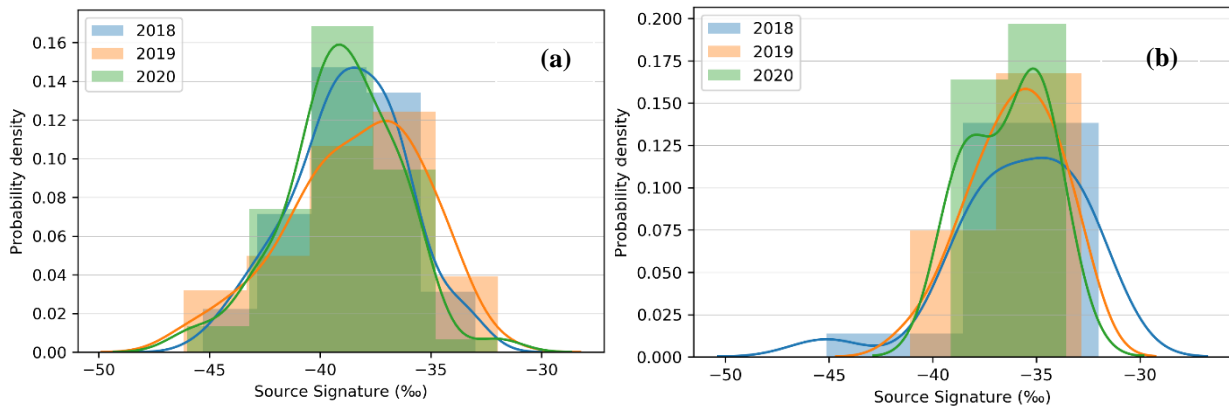


Figure 4a: 1-day window, where the average $\delta^{13}\text{C}$ was $-37.2 \pm 0.9\text{‰}$.

Figure 4b: 7-day window with average $\delta^{13}\text{C}$ of $-36.1 \pm 0.3\text{‰}$. Results from 2020 display a bimodal distribution of source signature values, whereas a normal distribution is seen in the 1-day window. This is likely due to the wider area of influence measured using the 7-day window, which could be measuring strong CO_2 signals from sources further away from the measurement site that is not observed in the 1-day window.

However, arguments could be made that the two-component mixing model that the Keeling plot results are based off are unable to accurately distinguish between anthropogenic sources and biogenic sources due to the similarities in the isotopic signatures of these sources.

Figure 5 shows the total summary of binned source signatures obtained from the 3-day time window analysis over the whole period between 2018-2020. The source signatures found over this period were within the range of -30.3‰ to -45.8‰ , with an average signature of $-36.8 \pm 0.5\text{‰}$. Two prominent peaks in the source signature distribution are present, first at $\sim -38\text{‰}$ and a second found at $\sim -36\text{‰}$. These signatures correspond to different sources from natural gas combustion, with the first more likely to be originating from domestic heating since this is expected to have a signature between -39‰ and -37‰ .

The results from the binned sources in figure 4a, figure 4b and figure 5, particularly due to the existence of two different modal signatures over the period 2018 – 2020, suggest that a mixture of sources due to the combustion of natural gas are the primary sources of CO_2 being detected at the measurement site. This would be in agreement with the outcomes from the emission map simulations ran by my peer, Yousuf Makki, who found that the combustion of fossil fuels proved to be the most dominating source of CO_2 . This was also found to be the case when calculations of the proportion of each source signature found from the Keeling plots showed that $\sim 48\%$ of the signatures could be attributed to natural gas combustion when a value of -36‰ was used for natural gas combustion.

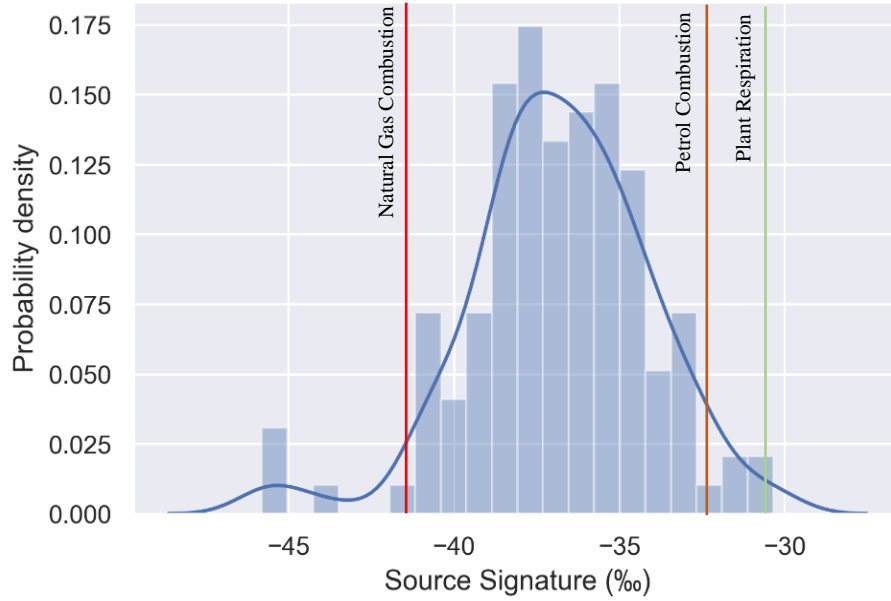


Figure 5: 3-day window binned signatures from the whole dataset shows that most of the isotopic signatures are confined within the natural gas combustion region. The coloured vertical lines provide rough classifications of each source, obtained from table 1, to enable an easier interpretation of the results

3.2 Time-Series Analysis of Source Signatures

Understanding the variations in CO₂ emissions from different sources over time was a significant area of study throughout this project. This subsection presents the results of the analysis performed over the whole period of which measurements were taken from using a 3-day window. The aim of this was to ultimately develop a better insight into how isotopic source signatures varied at different times throughout the year and understand the possible causes behind them.

A time series analysis of the source signature values across all three time windows showed consistent seasonal variation in $\delta^{13}C$ during afternoon periods. Figure 7a shows a well-defined cycle of source signature values obtained from the 3-day window analysis. Winter periods exhibited the greatest range of variations in observed $\delta^{13}C$, but a distinct shift towards heavier signatures can be seen via the higher average $\delta^{13}C$ value during the winter. This is supported by Patiki et al, in their study of the seasonal isotopic composition cycle of CO₂ [4], where results indicated a larger impact of natural gas combustion on the signatures during the winter. Whilst the lighter signatures are more prevalent across the summer, with an average signature of $-34.4 \pm 0.6\text{‰}$ which would be expected as a result of the increased emissions from plant respiration, this result is likely affected by the heatwaves experienced in 2019 which produced some of the warmest days on record. The hottest winter day reached 21.2°C and the hottest day ever recorded occurred in July at 38.7°C, as well as several other days with above average temperatures throughout 2019 [10].

One of the other probable effects of the warmer weather on the source signature cycle is the reduced influence of signatures from the use of domestic heating for example. The signature for the combustion of natural gas used for domestic heating is likely to be towards the middle of the natural gas combustion range $\sim -37\text{‰}$ which can be observed from the absence of signatures found around this mark from figure 7a during summer periods. During the winter, the combustion of fossil fuels for heating are most likely to be the key source of natural gas combustion, which would imply that the signature associated with domestic heating is likely to fall between -39‰ and -37‰ , this would be supported by the fact that the average isotopic signature over the winter was found to be $-37.6\pm0.4\text{‰}$. The conclusion of temporal variations leading to increased influence from biogenic emissions on the over trend of observed $\delta^{13}\text{C}$ was also found to be the case in the diurnal study of atmospheric CO_2 in south-west London between 2000-2012 by David Lowry et al [23].

The average source signature over 2019 was $-35.7\pm0.5\text{‰}$ – lower than the average $\delta^{13}\text{C}$ of 2018, $-36.8\pm0.4\text{‰}$ and 2020 $-36.2\pm0.4\text{‰}$. However, it could be argued that the effects of the recent lockdown were likely to distort the averages for 2020 when trying to understand the source signature cycle. As will be shown in section 3.3, it was found that there was a slight reduction in lighter isotopic signatures most likely due to the reduced amounts of petrol combustion from road traffic on the overall signatures found between March and June for 2020. It would therefore be reasonable to expect a dissimilar trend from spring onwards in the 2020 signatures, with potentially more frequent heavier source signatures relative to 2018 and 2019. This can be seen to an extent in Figure 7a, where between 2020-01 and 2020-06, the signatures follow a similar trend to that of the corresponding months for 2018 and 2019 but to understand these implications better, the data collected beyond June would need be studied to perceive any long-lasting effects in the overall trend of signatures for 2020.

Comparisons between figure 7a and 7b show a clear relationship between concentrated regions of natural gas combustion with greater spikes in CO_2 concentration (most frequently during the winter), further suggesting that the detected pollution events are mostly due to natural gas burning. CO_2 concentrations are enriched during the winter periods and significantly lower during the summer, which is due to boundary layer dynamics at these times. The boundary layer is generally lower at night and stays low for extended periods during the winter and could lead to the biosphere acting as a source of CO_2 during the day as well as the night due to reduce exposure to sunlight. It is likely therefore that these concentrations feed over into the measured afternoon concentration and this is what is causing the variations during winter periods. These results indicate a mixture of sources from the combustion of natural gas as the main driver behind the observed seasonal cycle of $\delta^{13}\text{C}$ with most of the observed signatures confined within the natural gas combustion range. Although identifying precisely the exact source of each observed signature requires further research into atmospheric CO_2 to aid in constraining the isotopic signatures more accurately.

Season	Range of Isotopic Signatures	Average Isotopic Signature
Summer	$-45.1\text{‰} - -30.3\text{‰}$	$-34.4\pm0.6\text{‰}$
Autumn	$-40.8\text{‰} - -31.5\text{‰}$	$-36.4\pm0.4\text{‰}$
Winter	$-46.8\text{‰} - -31.7\text{‰}$	$-37.6\pm0.4\text{‰}$
Spring	$-43.7\text{‰} - -30.4\text{‰}$	$-35.5\pm0.5\text{‰}$

Table 2: Summary of $\delta^{13}\text{C}$ results according to the meteorological seasons from a 3-day window analysis. A pattern of lighter isotopic source signatures during colder seasons and heavier signatures during the winter can be seen from the average isotopic signature values.

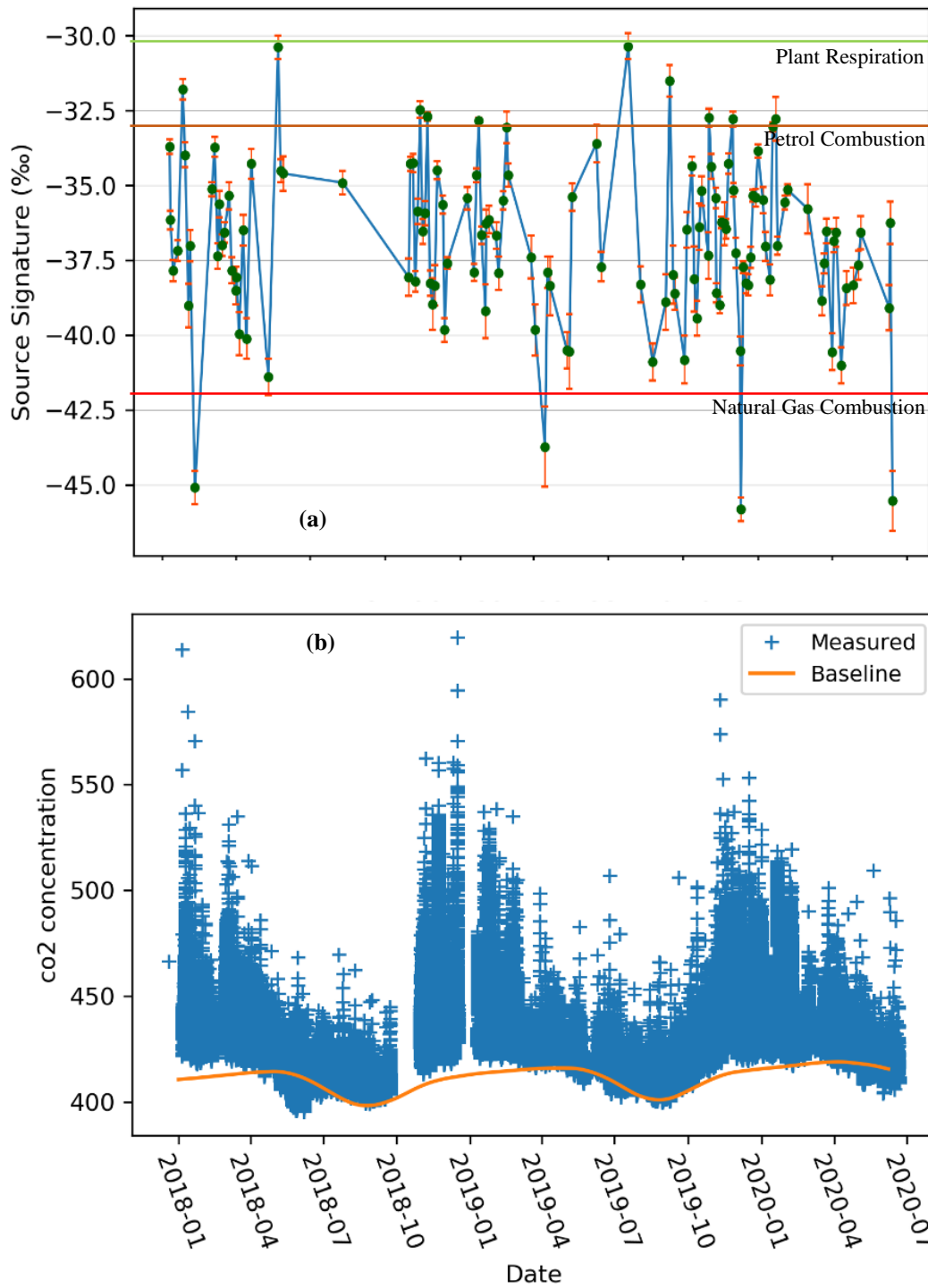


Figure 7a: Time series of isotopic source signatures. A strong seasonal cycle of a greater cluster of $\delta^{13}\text{C}$ from within the natural gas combustion range across winter and autumn seasons can be observed. Uncertainty values on the isotopic signatures ranged between 0.2‰ and 0.7‰.

Figure 7b: Measured afternoon CO₂ concentration in ppm, with the baseline concentration measured from Mace Head, Ireland. The plot of measured CO₂ concentrations also shows a strong seasonal pattern, with depleted concentration observed during the summer and higher concentrations during the winter as was found from researchers at Royal Holloway University [23].

NB. The format of the date axis is Year-Month

3.3 Analysis of the Lockdown Period

Data from the lockdown period spanning 23rd March – 23rd June was analysed to understand the implications on the $\delta^{13}\text{CO}_2$ cycle of the recent lockdown that was implemented across the UK. The lockdown measures limited the amount of urban activity by implementing a temporary closure to all non-essential stores and discouraging non-essential travel. Naturally, restricted levels of urban activity in this way would be expected to have a direct impact on CO_2 emissions and greenhouse gas emissions in general. To understand the how the lockdown affected the source signature variations, it is useful to look at the corresponding time periods for the previous years and draw more meaningful conclusions. The aim of this was to examine whether the lockdown measures would cause the variations in CO_2 source signatures in 2020 to diverge from previously observed fluctuations or if the same seasonal variation would still occur.

Figure 8 represents a time series of the data collected between the 1st March – 23rd June for each year since 2018, using a 3-day window. The 3 weeks prior to lockdown were included in these results since the effects of the lockdown were likely to take some time to impact the results, considering the $\delta^{13}\text{C}$ variations before this period allows for the changes caused by the lockdown to be understood in the context of greater than average sunlight exposure, heat and reduced rainfall [26]. Analysis using 7-day windows were not implemented, this was in part due to the lockdown period only extending across 98 days and the use of a 7-day window did not allow enough isotopic source signatures to be calculated, hence making any significant conclusions difficult to produce. However, from the 3-day window analysis the lockdown signatures appear to follow a trend similar to that of the data from 2018 and 2019 but covering a notably larger range of source signature values with $\delta^{13}\text{C}$ values between -43‰ to -29.7‰ .

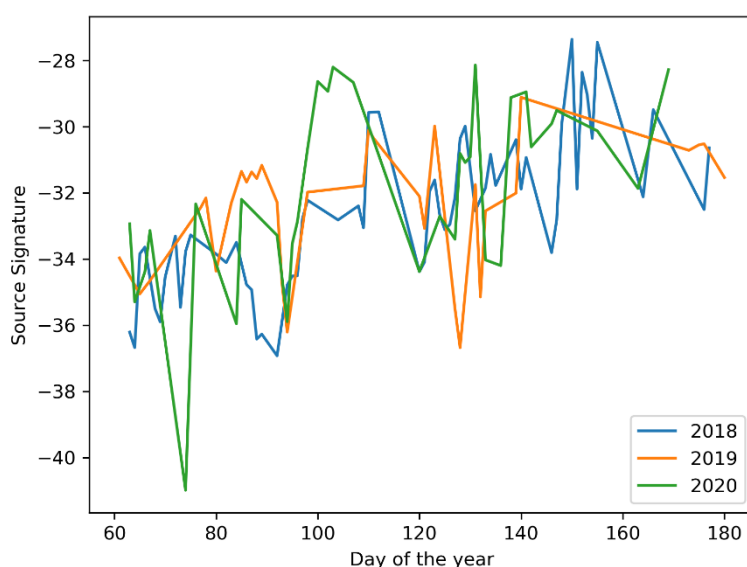


Figure 8: Time series of source signature values (‰) throughout the lockdown period using a 3-day time window. Results show a greater range of $\delta^{13}\text{C}$ in the 2020 cycle, but a similar upward trend towards lighter signatures can be clearly be observed.

Analysis using 3-day windows only produced 107 source signatures. Due to the limited number of isotopic signatures obtained from the lockdown period, it can be difficult to categorically explain the variations observed with complete confidence. But the influence of heavier signatures in 2020, particularly during late March and early April can be seen plainly. The most likely cause of this could be attributed to the reduction in vehicle use early on during the lockdown, leading to fewer CO₂ emissions from petrol combustion, resulting in less of an impact from lighter signatures corresponding to values between -32‰ and -31‰. This is observed in the histogram plot of figure 9 where significant contributions from lighter source signatures below -31‰ can be observed in 2020. This can also be seen from the calculations of the average isotopic source signature for each year during the lockdown months, which for 2020 was -32.1 ± 0.8 ‰ lighter than the values for 2019, -33.2 ± 0.3 ‰ and 2018, -35.7 ± 1.8 ‰, all of which are lighter than the average $\delta^{13}\text{C}$ found for each year in the previous section. Although, it would be reasonable to expect less of a presence of signatures around -32‰ if there is less petrol combustion contributing to CO₂ emissions measured in an air sample, which can be seen from the fewer number of signals corresponding to petrol combustion in the 2020 plot when compared against 2018 and 2019 levels. A possible explanation for these observations could be due to the higher average temperatures that accompany the spring and summer periods over which the nationwide lockdown took place, which can be seen from the increase of signatures below -30‰. This would be supported by the upward trend of the signatures shown in figure 8 which illustrate how the transition across spring into summer leads to the prominence of lighter source signatures due the increased contribution from biogenic respiration and this factor dominates over the petrol combustion signatures.

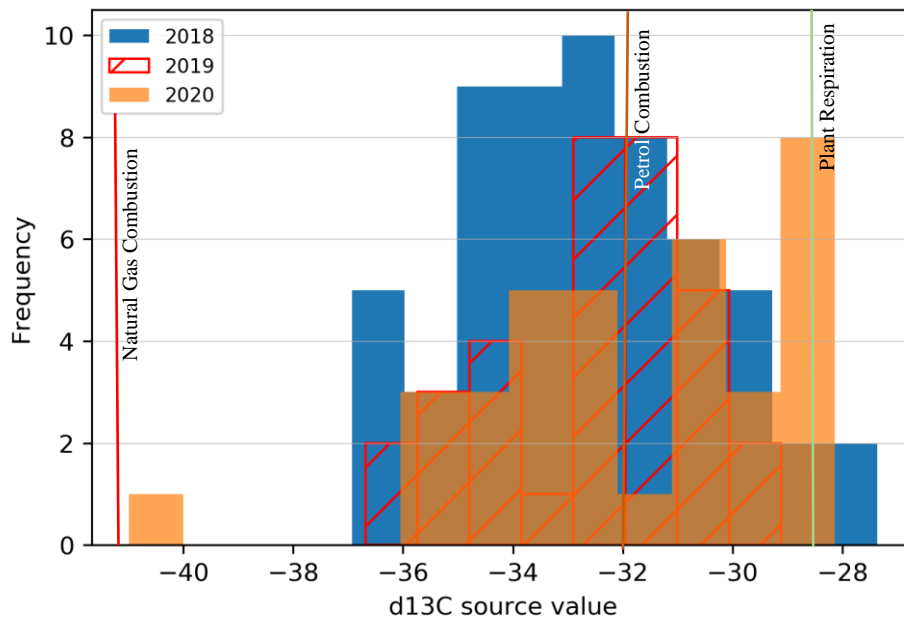


Figure 9: Binned plot of the observed signatures and corresponding number of events observed for each isotopic source signature using a 3-day time window. Fewer signatures corresponding to sources of petrol combustion are seen in 2020, with the biosphere contributing significantly throughout the spring period of 2020 which could potentially be due to the relatively warm spring experienced this year. In creating this histogram plot for $\delta^{13}\text{C}$, data calculated between 23rd – 23rd June were used.

3.4 Wind Data Analysis

This project has focused on understanding the variations in the isotopic source signatures of CO₂ over afternoon periods. Naturally, wind conditions contribute to driving the variations in CO₂ concentrations and affect the travel routes for air samples arriving at the sensor. This makes wind conditions an important aspect to consider when investigating the different source signatures observed. The wind direction varies greatly over diurnal periods, so it was important to consider how this might possibly be impacting the variation in $\delta^{13}\text{C}$ cycles, since the analysis in this project was mostly concerned with afternoon variations.

Part of this project looked to try and establish a relationship between the measured source signatures and the atmospheric processes that bring this to the weather station. A study by David Lowry et al, on methane emissions in London found that shifts in isotopic signatures are strongly influenced by wind direction [9], with west/north-westerly winds being associated with carbon-13 enrichment. This section discusses the results found from examining the wind direction data and the possible effects it had on the observed signatures.

Only 3-day windows and 1-day windows were used when studying the wind direction. Initially the average wind direction over specified time periods was calculated and compared against the corresponding source signature results generated from the Keeling plots. This was found to be an ineffective way of understanding wind direction as a driver of isotopic signature variation, as wind direction generally varies greatly over diurnal periods and even more so at lower wind speeds. Taking the average wind direction also raised further issues when calculating results over longer time periods and was likely to generate ill-defined directions [25]. Instead, the mode wind direction over the same length as the corresponding window was used. However, working with wind direction data in this way was challenging and will inevitably lead to some bias in the results, which is assumed to be the case in the findings here.

Since just half the data was collected for 2020, only 2019 and 2018 data were used in the analysis of wind direction and isotopic source signatures. Figure 10 and figure 11 show a series of polar plots that summarise the findings from the analysis of the 1-day and 3-day time windows, constructed using the windrose version 1.4 package on python. In creating the windrose plots, the source signatures from the Keeling plots were recorded with the date(s), from which the wind direction data was then filtered out based on the corresponding date from the Keeling plot results. There are notable similarities observed in each of the windrose plots for both time windows, which suggest that most of the signatures found seem to predominantly arise from locations towards either the east or west. From the plots, it can be seen that natural gas combustion source signatures between -33‰ and -36‰ tend to be more prevalent from the east during 2018 in both the 3-day and 1-day time windows. Wind sector analysis at Royal Holloway University was able to show that winds from easterly and south-easterly directions were associated with greater CO₂ concentrations during 2000 – 2012 [23] and from the time series plot of afternoon CO₂ concentrations in figure 7b, higher CO₂ concentrations were found to mainly be due to increased combustion of natural gas. This would suggest that a significant amount of CO₂ pollution events was the result of increasing natural gas combustion from eastern regions.

As would be expected from the plots of the 1-day window in figure 10, a greater dispersion of signatures across different directions is displayed, however the results from the 1-day window analysis may act as a good indicator as to the locations of nearby sources. Around the campus in which the weather station is deployed, there are a handful of potential local CO₂ sources contributing to the total emissions, including a power station located east of the weather station and small tree garden type environments. However, the plots from 2019 show that the

signatures between -33‰ and -36‰ largely arise from the west and less so from the east, which would suggest that the isotopic signatures within this range alone cannot quite be attributed to the on-campus power station. It should be noted that signatures from the power station were likely only found during its running and operating times which may have been changed on different days and could explain any discrepancies found from natural gas combustion signatures of the power station at different times. However, isotopic signatures at the heavier end of the natural gas combustion range were not as represented in the windrose plots, most likely due to the dominance of lighter natural gas combustion signatures, as a result nothing conclusive can be said about these heavier signatures.

The general dispersion of the $\delta^{13}C$ values found from analysing the wind direction data would suggest that any given sample of air, is likely to consist of a mixture of different sources being observed. This is more apparent over the 3-day window where distinct signatures cannot be attributed to specific directions, for instance sources between -35.4‰ – -38‰ in 2019 appear evenly distributed over western directions, which makes it difficult to conclusively explain the variations of specific signatures over time.

Given that both wind speed and wind direction data was collected, an improved approach to understanding the effects of wind conditions on the source signature cycle could be to represent both of these quantities as vector components [25]. From this, calculations of the resultant average wind direction along with the scalar average wind speed are likely to better define source signature directions. Previous studies in meteorology involving wind data have adopted this approach, but due to time constraints this was not possible here.

Another interesting aspect that was not explored in this section but could potentially provide a better insight into the effects of wind direction on CO₂ source signatures, would be to investigate the variation of source signatures and wind direction over the different seasons. Analysing the wind direction data over shorter periods could allow for better containment of local atmospheric CO₂ sources and how they vary with patterns of atmospheric transport. For example, during the winter seasons, the average $\delta^{13}C$ are significantly heavier than during the rest of the year. Analysing the wind direction and isotopic signature during these periods could potentially reveal variations of heavier natural gas signatures that were not obtainable from the yearly plots.

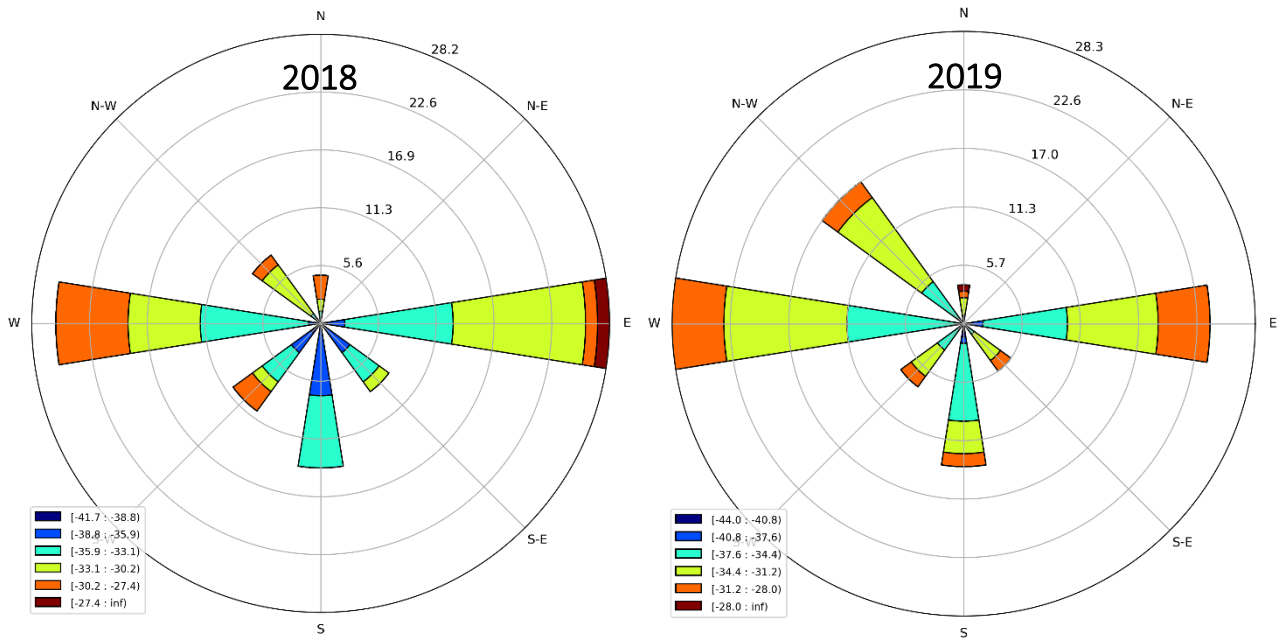


Figure 10: 1-day window windrose plots. Signatures appear more dispersed across the 1-day window, with smaller contribution from southerly directions. This would be expected due to the nature of varied wind directions throughout a short time period.

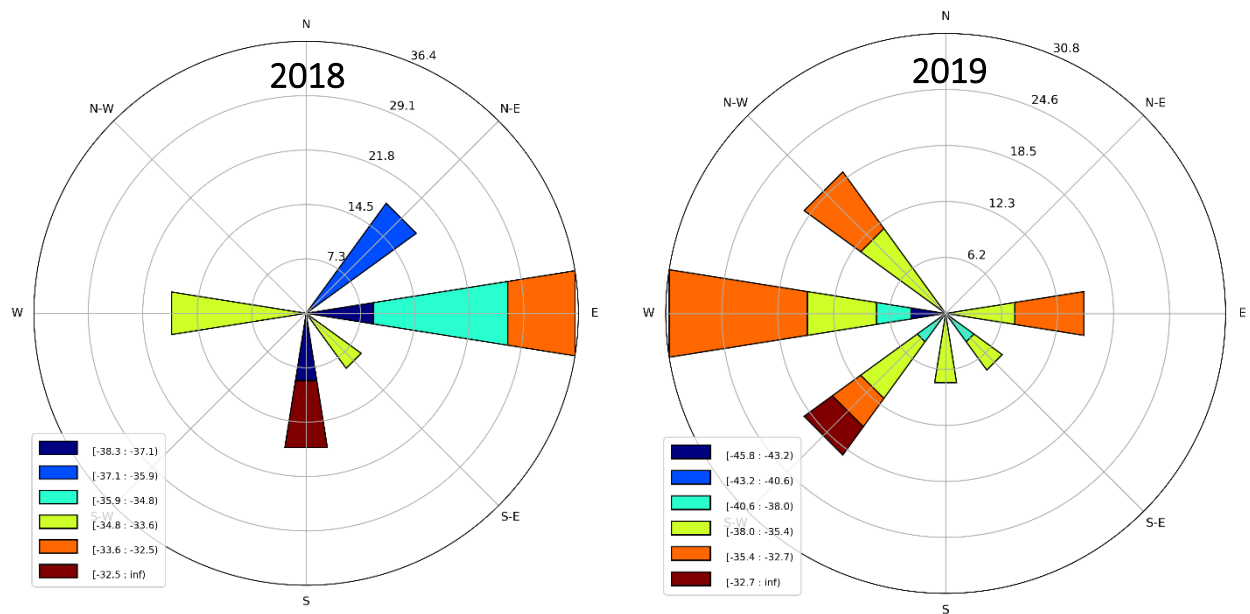


Figure 11: 3-day windrose plots. Signatures found in 2019 show disagreement with the 1-day plot of 2019 with heavier signatures dominated from western regions. The 2018 plot shows that $\delta^{13}\text{C}$ of $\sim -33\text{‰}$ are more prevalent from the east whilst in 2019 it is more dispersed but predominantly from the west. The legend located at the bottom left of each windrose plot represents the signature value for the corresponding segment

Conclusion

To understand the source of anthropogenic CO₂ source measured in London, the isotopic source signatures of carbon-13 in atmospheric CO₂ were studied. The use of isotope ratios together with CO₂ concentration measurements has become a widely adopted method to determine the isotopic signature of a CO₂ source. The results of this project and several other studies have proved that a greater understanding of isotopic source signatures of CO₂ is severalfold. As well as quantifying the strength of local sources in the atmosphere, the use of isotopic signatures observations enables improvement of existing atmospheric transport models and allows for better constraints to be placed on source signatures – which will ultimately go some way in assisting to address the climate consequences as a result of increasing anthropogenic CO₂ emissions.

The isotopic composition of the CO₂ measured in London was derived through the application of the Keeling plot method over 7-day, 3-day and 1-day time windows, to understand the variations in the sources observed. Qualitative analysis of the results showed that the dominating signatures found were from a mixture of sources arising from the combustion of natural gas. The source signatures generally showed a clear and consistent cyclical pattern across all three time windows, where winter seasons displayed heavier signatures at an average value $-37.6 \pm 0.4\text{‰}$ and summer periods exhibiting slightly lighter average values $-34.4 \pm 0.6\text{‰}$ over the whole dataset, with the signatures showing less variability during the winter, as opposed to summer periods which had a larger range of $\delta^{13}\text{C}$. The main driver behind these differences was attributed to the dominance of different sources throughout the year primarily as a result of varying temperatures and sunlight exposure. Biospheric CO₂ emissions were found to contribute most significantly during the summer and spring as a result of increased plant and soil respiration, which corresponded to signature values between -30‰ – -26‰ . Whereas during the winter, greater contributions from heavier signatures of natural gas combustion were observed largely due to the burning of natural gas being the leading source of domestic heating in the UK. Comparisons of the time series of CO₂ concentration and $\delta^{13}\text{C}$ variations showed a clear relationship of increased pollution events with greater natural gas combustion. From this, the seasonal changes in urban consumption of fossil fuels are clearly revealed from the measurements of atmospheric CO₂.

The lockdown period over the spring was analysed to understand the effects of human activity on CO₂ emissions in London by comparing the lockdown measurements against the spring months of 2018 and 2019. The results showed that the isotopic source signatures between the 23rd March 2020 and 23rd June 2020 generally followed a similar trend to the corresponding months of 2018 and 2019, trending towards lighter signatures near the end of Spring. However, the data from 2020 displayed greater variation, where notable spikes beyond the general trend in signatures occurring periodically, with peak $\delta^{13}\text{C}$ reaching -27.8‰ in the lockdown during early April. The average $\delta^{13}\text{C}$ for 2020, $-32.1 \pm 0.8\text{‰}$ was shifted towards lighter signatures, near the lighter end of the petrol combustion range – implying that the reduction in road traffic most likely had a direct impact of reducing the influence petrol combustion on the overall source signatures. Further inspection of the data beyond the lockdown period should be carried out to deduce whether the lockdown produced any significant changes on the overall seasonal cycle of $\delta^{13}\text{C}$ and how urban activities could be responsible for this.

Analysis of the wind direction data showed that lighter natural gas combustion source signatures were originating from easterly directions in 2018 and mainly from the west in 2019. The windrose plots from the 1-day windows were constructed to understand the variations found from the local sources. Analysis showed that a similar distribution of source signatures

between -33 and -36 were coming from the east and west. Signatures at the heavier end of the natural gas combustion did not seem as well represented in the windrose plots and a similar case for signatures corresponding to plant and soil respiration. This would further suggest that the main contributing source of atmospheric CO₂ is due to a mixture of sources from the burning of natural gas.

Outlook

As a mainly data-orientated project, there were certain aspects of the measured carbon dioxide data that could have been explored further which was not possible due to time constraints. To develop on the results found thus far, analysis over short windows could reveal greater detail about source signature variations. The results found in the analysis of the afternoon periods using 1-day, 3-day and 7-day windows all showed strong influence of the biosphere on the total emissions. Looking at hourly windows spanning whole day periods could allow an independent inspection of periods where specific anthropogenic sources of CO₂ are likely to dominate. For instance, taking hourly time windows during rush hour periods and assessing whether biospheric sources still have a large influence or if petrol combustion signatures would contribute more significantly. This would involve calculating isotopic source signatures by constructing Keeling plots for each hour in a specified window, which could be narrowed down further to half hourly window, 15-minute windows and so on. Essentially, reducing window lengths to observe the CO₂ concentration and ¹³C cycles formed over shorter periods and comparing against the longer time windows.

Another aspect that any future work could focus on is to inspect the isotopic source signatures over weekdays relative to weekends and bank holidays. Establishing weekday cycles provides a better insight into the variability of dominant sources of atmospheric CO₂ emissions at different periods of peak urban activity.

References

1. Kristal R. Verhulst, Anna Karion, Joil Kim, et al. (2017). Carbon dioxide and methane measurements from the Los Angeles Megacity Carbon Project – Part 1: calibration, urban enhancements, and uncertainty estimates. doi.org/10.5194/acp-17-8313-2017
2. Thomas Röckmann, Simon Eyer, et al. (2016). In situ observations of the isotopic composition of methane at the Cabauw tall tower site. doi.org/10.5194/acp-16-10469-2016
3. <https://www.gov.uk/government/statistics/final-uk-greenhouse-gas-emissions-national-statistics-1990-to-2018> - retrieved on 21/09/2020
4. D. E. Pataki, D. R. Bowling, et al. (2003). Seasonal cycle of carbon dioxide and its isotopic composition in an urban atmosphere: Anthropogenic and biogenic effects. doi.org/10.1029/2003JD003865
5. Stefani Venturi, Franco F. Tassi, et al. (2019). Seasonal and diurnal variations of greenhouse gases in Florence (Italy): Inferring sources and sinks from carbon isotopic ratios. doi.org/10.1016/j.scitotenv.2019.134245
6. D. E. Pataki, J. R. Ehleringer, et al. (2003). The application and interpretation of Keeling plots in terrestrial carbon cycle research. doi.org/10.1029/2001GB001850
7. Charles D. Keeling. (1958). The concentration and isotopic abundances of atmospheric carbon dioxide in rural areas. doi.org/10.1016/0016-7037(58)90033-4
8. Jonathan M. Frantz, Nilton N. Cometti, Burce Bugbee. (2004). Night Temperature has a Minimal Effect on Respiration and Growth in Rapidly Growing Plants. doi.org/10.1093/aob/mch122
9. David Lowry, Craig W. Holmes, Nigel D. Rat. (2001). London methane emissions: Use of diurnal changes in concentration and $\delta^{13}\text{C}$ to identify urban sources and verify inventories. doi.org/10.1029/2000JD900601
10. <https://www.metoffice.gov.uk/about-us/press-office/news/weather-and-climate/2019/weather-overview-2019> - retrieved on 29/09/2020
11. Lana Cohen, Detlev Helmig, et al. (2007). Boundary-layer dynamics and its influence on atmospheric chemistry at Summit, Greenland. doi.org/10.1016/j.atmosenv.2006.06.068
12. P. T. Boggs and J. E. Rogers. (1990). Statistical analysis of measurement error models and applications. Contemporary Mathematics, vol. 112, pg. 186
13. <http://www.sp.ph.ic.ac.uk/~hgraven/research.html> - retrieved on 28/09/2020
14. Stephanie C. Pugliese, Jennifer G. Murphy, et al. (2017). Characterization of the $\delta^{13}\text{C}$ signatures of anthropogenic CO_2 emissions in the Greater Toronto Area, Canada. doi.org/10.1016/j.apgeochem.2016.11.003
15. Thomas Esch, Wieke Heldens, Andreas Hirner, et al. (2017). Breaking new ground in mapping human settlements from space – The Global Urban Footprint. doi.org/10.1016/j.isprsjprs.2017.10.012
16. Vincent J. Hare, Emma Loftus, et al. (2018) Atmospheric CO_2 effect on stable carbon isotope composition of terrestrial fossil archives. doi.org/10.1038/s41467-017-02691-x
17. Shanno T. Clark-Thorne, Crayton J. Yapp. (2003) Stable carbon isotope constraints on mixing and mass balance of CO_2 in an urban atmosphere: Dallas metropolitan area, Texas, USA. doi.org/10.1016/S0883-2927(02)00054-9
18. D. Widory. (2006). Combustibles, fuels and their combustion products: A view through carbon isotopes. doi.org/10.1080/13647830600720264
19. Maria Dios, et al. (2012). A mixed top-down and bottom-up methodology in spatial segregation of emissions based on GIS tools. doi.org/10.2495/AIR120201

20. Mirosław Zimnoch, Tadeusz Florowski, Jarosław M. Necki, et al. (2007) Diurnal variability of $\delta^{13}\text{C}$ and $\delta^{18}\text{O}$ of atmospheric CO_2 in the urban atmosphere of Kraków, Poland. doi.org/10.1080/10256010410001670989
21. David Widory, Marc Javoy. (2003). The carbon isotope composition of atmospheric CO_2 in Paris. doi.org/10.1016/S0012-821X(03)00397-2
22. Euan Nisbet, Ray Weiss. (2010). Top-Down Versus Bottom-up. doi.org/10.1126/science.1189936
23. Ivan Y. Hernández-Paniagua, David Lowry, et al. (2005). Diurnal, seasonal, and annual trends in atmospheric CO_2 at southwest London during 2000-2012: Wind sector analysis and comparison with Mace Head, Ireland. doi.org/10.1016/j.atmosenv.2015.01.021
24. P. Thunis, B. Degraeuwe, K. Cuvelier, et al. (2016). A novel approach to screen and compare emission inventories. doi.org/10.1007/s11869-016-0402-7
25. Stuart K. Grange. (2014). Technical note: Averaging wind speeds and directions. doi.org/10.13140/RG.2.1.3349.2006
26. <https://www.carbonbrief.org/met-office-why-2020-saw-a-record-breaking-dry-and-sunny-spring-across-the-uk> - retrieved on 28/09/2020
27. Rebeca Santamaria-Fernandez and Thierry Le Goff. (2010). Isotopic characterisation of in-house purified progesterone for $^{13}\text{C}/^{12}\text{C}$ isotope ratios by multicollector ICP-MS. doi.org/10.1039/b922642g
28. John B. Miller, Pieter P. Tans. (2003). Calculating isotopic fractionation from atmospheric measurements at various scales. doi.org/10.1034/j.1600-0889.2003.00020.x